## 4.2 SPATIAL VARIABILITY OF TURBULENCE CHARACTERISTICS IN AN URBAN ROUGHNESS SUB-LAYER

Giap Huynh*, Sam Chang, Cheryl Klipp, Chatt Williamson, Dennis Garvey, and Yansen Wang
U.S. Army Research Laboratory, Adelphi, Maryland, 20783

**ABSTRACT**

We present the results of sonic data analyses from Army Research Laboratory's five meteorological tower measurements during Joint Urban 2003 (JU2003) field campaign. Conducted in Oklahoma City in the summer of 2003, the JU2003 was a cooperative undertaking to study transport and diffusion in the atmospheric boundary layer in an urban environment. This paper focuses on the spatial variability of turbulence characteristics in an urban roughness sub-layer observed in metropolitan area of Oklahoma City. Inter-comparisons of turbulence statistics computed from the sonic anemometer data collected at the five tower locations, as well as between urban and suburban areas demonstrate significant heterogeneity of turbulence characteristics in the urban roughness sub-layer. Comparisons between our results and similarity formulations are also presented. Local scaling and similarity theory appear very difficult to apply to the urban roughness sub-layer.

### 1. INTRODUCTION

The Joint Urban 2003 was a cooperative undertaking to study transport and diffusion in the atmospheric boundary layer in an urban environment. It was conducted in Oklahoma City in the summer of 2003 (Allwine *et al*., 2004). The Army Research Laboratory (ARL) deployed a number of measurement facilities, including an array of sonic anemometers mounted on five meteorological towers in the metropolitan area (see Yee *et al*. (2004) for detailed information on the ARL measurements). The large amount of sonic data was processed using available quality control software (Vickers and Mahrt, 1997).

Various turbulence characteristics have been computed and analyzed. This paper focuses on the analysis of turbulent fluxes, drag coefficient, turbulence variances and intensities in the urban roughness sub-layer. Other results, including spectral analyses of $u, v, w$, and $T$ in urban and suburban locations, have been presented elsewhere (Chang *et al*., 2004; Garvey *et al*., 2004; Klipp *et al*., 2004).

### 2. DATA COLLECTION AND PROCESSING

Ultrasonic anemometers (R. M. Young, Model 81000) were mounted on towers of ten meter height at three levels (10 m, 5 m, and 2.5 m above the ground) for Towers #2 and #3 and at two levels (10 m and 5 m) for Towers #1, #4, and #5. Instruments below the 10 m level were mounted due south of the towers at the end of 2 m booms in anticipation of the prevailing southerly winds in Oklahoma during the summer. For 5m and 2.5m sonics, only the data with wind direction from $90^o$ to $270^o$ are used in order to avoid any of "tower shadow effects". Anemometer elevations (heights above the ground) were accurate to about +/- 0.1 m for 10.0m and 5.0 m instruments, and about +/- 0.05 m for the 2.5 m instruments. Figure 1 shows the locations and immediate surroundings of these 5 towers. As indicated in Figure 1(b), the immediate vicinity around Tower #1 is quite open; there were no houses or trees within a distance of 50 m except for a small portable trailer (3.3 m in height) to the south-southwest. There were a number of buses with a height of about 3.5 m to the west of the tower. The average height of houses in the surrounding area was estimated to be about 6 m. Tower #2, on the other hand, was surrounded by industrial buildings with an average height of 10 m within a distance of 30-50 m, as indicated by Figure 1(c). Tower #3, Figure 1(d), has an open fetch to the south, and the ground slopes off in this direction. There are trees with heights of 10-15 m east and west of the tower, with a small house near the trees to the east. As seen from Figure 1(e), Tower #4 was located near a highway, with a school building on the west and open ground for distances more than 50 m north, east, and south. Figure 1(f) shows that Tower #5 was surrounded by buildings on the east, south and west sides, with building heights between 6-8 m. There was a line of fairly tall trees across the alley to the north.

Generally speaking, Towers #2 and #5 can be considered typical of industrial or warehouse urban areas while the other three tower locations typify suburban areas. Lundquist *et al.* (2004) have estimated the mean building height for the urban area of Oklahoma City as 5-15m. Measurements by our sonic anemometers, conducted outside the central business district, can therefore be considered to represent the urban roughness sub-layer (Roth, 2000) at specific locations. The sonic anemometer data consist of three wind components ($u, v, w$) and sonic temperature ($T$). The sampling rate of the sonic anemometers was 10 Hz. For sonic anemometer tilt correction, the traditional two angle rotation method (Kaimal and Finnigan, 1994) was used for each time series of 30 minutes (18000 data points). After the tilt correction, the three components of the wind vector are $u$ (streamline), $v$ (transverse), and $w$ (normal) with

* *Corresponding author address:* Giap Huynh, U.S. Army Research Laboratory, AMSRD-ARL-CI-EE, Adelphi, MD 20783; e-mail: huynh@arl.army.mil

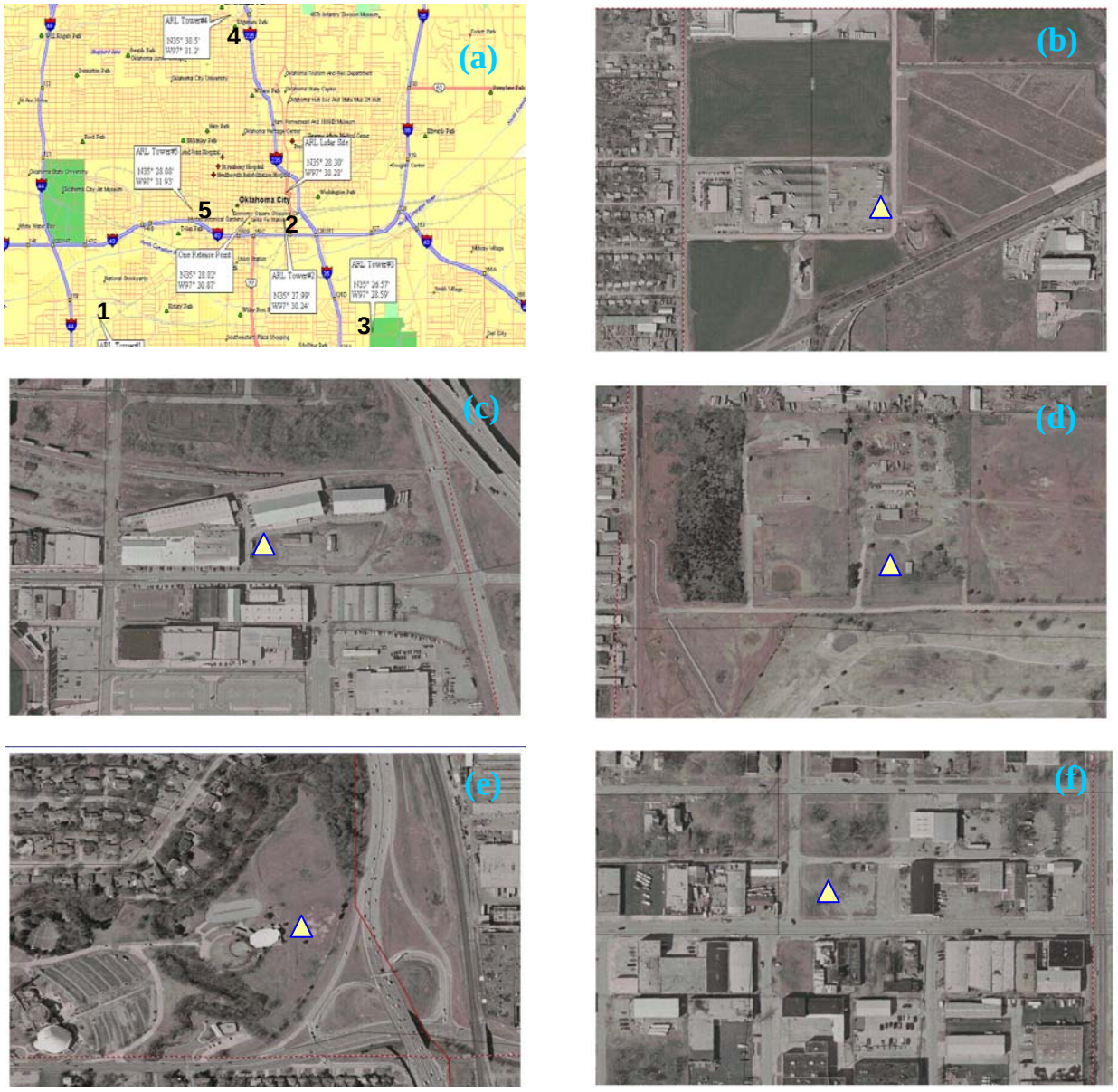


**Figure 1.** Locations (a) and surroundings of the ARL 5 meteorological towers indicated by triangles. Aerial photos for Tower No. 1 (b), No. 2 (c), No. 3 (d), No. 4 (e), and No. 5 (f) were obtained from U.S. Geological Survey, EROS Data Center, Sioux Falls, SD. (http://seamless.usgs.gov)

$\bar{v} = \bar{w} = 0$, where the over-bar indicates the 30-minute average. For our analysis we adopted the Analysis Package for Time Series (APAK) developed at Oregon State University by Vickers and Mahrt. (http://blg.coas.oregonstate.edu/Software/software.html)

## 3. SURFACE LAYER SIMILARITY FORMULATION

For a canopy flow, the traditional surface layer (Monin-Obukhov) similarity formula for the non-dimensional wind shear can be expressed as

$$\phi_m = \frac{k(z-d)}{u_*}\frac{d\bar{u}}{dz} \qquad (1)$$

where $\bar{u}$ is the mean wind speed at the height $z$ above the ground, $d$ the displacement height, $k$ the Von Karman constant (0.4), and $u_*$ the friction velocity

$$u_* = \left[\left(\overline{u'w'}\right)^2 + \left(\overline{v'w'}\right)^2\right]^{1/4} \qquad (2)$$

where the variables with prime ($u', v', w'$) refer to the three turbulent wind components. Integration of (1) results in the non-dimensional wind profile which is related to the drag coefficient ($C_d$)

$$C_d^{-\frac{1}{2}} = \frac{\bar{u}}{u_*} = k^{-1}\left[\ln\left(\frac{z-d}{z_0}\right) - \psi_m(\zeta')\right] \qquad (3)$$

with $\zeta' = \frac{(z-d)}{L}$ (4)

where $z_0$ is the roughness length, $L$ the Obukhov length

$$L = \frac{-u_*^{\,3}}{\left[k\left(\frac{g}{\bar{T}}\right)H\right]} \qquad (5)$$

where $g$ is the acceleration of gravity (9.81 $ms^{-2}$), $H$ (= $\overline{w'T'}$) the kinematic heat flux, $\bar{T}$ the mean air temperature, and $\psi_m$ in (3) the correction to the logarithmic wind profile for diabatic conditions.

$$\psi_m = \ln\left[\left(\frac{1+x^2}{2}\right)\left(\frac{1+x}{2}\right)^2\right] - 2\tan^{-1}(x) + \frac{\pi}{2} \qquad (6a)$$

$$x = (1-15\zeta')^{1/4} \quad \text{for } \zeta' < 0 \qquad (6b)$$

and $\psi_m = -5\zeta'$ for $\zeta' > 0$ (7)

The normalized standard deviation of longitudinal ($\sigma_u = \sqrt{\overline{u'^2}}$), transverse ($\sigma_v = \sqrt{\overline{v'^2}}$), vertical ($\sigma_w = \sqrt{\overline{w'^2}}$) wind velocity components, and temperature ($\sigma_T = \sqrt{\overline{T'^2}}$) can be written for unstable conditions ($\zeta' < 0$)

$$\frac{\sigma_j}{u_*} = C_{j1}\left[1 - C_{j2}\zeta'\right]^{1/3}, \quad j = u, v, w \qquad (8)$$

$$\frac{\sigma_T}{T_*} = -C_{T1}\left[1 - C_{T2}\zeta'\right]^{-1/3} \qquad (9)$$

and for stable conditions ($\zeta' > 0$)

$$\frac{\sigma_j}{u_*} = C_{j3}, \quad j = u, v, w \qquad (10)$$

$$\frac{\sigma_T}{T_*} = C_{T3} \qquad (11)$$

where the temperature scale

$$T_* = -\frac{H}{u_*} = -\frac{\overline{w'T'}}{u_*} \qquad (12)$$

For neutral condition ($L \to \infty, \zeta' \to 0, \psi_m \to 0$)

$$C_{j1} \sim C_{j3}, \quad \zeta' \to 0 \qquad (13)$$

$$C_{T1} \sim C_{T3}, \quad \zeta' \to 0 \qquad (14)$$

The experimental constants ($C_{j1}, C_{j2}, C_{j3}, C_{T1}, C_{T2}, C_{T3}$) in the above equations have been evaluated by many individual measurements; see Sobjan (1989), DeBruin *et al*. (1993), and Roth (2000) for example. Over flat terrain, the estimated values are approximately (Panofsky and Dutton (1984), and Tillman (1972))

$$C_{u1} \approx C_{u3} = 2.4, \quad C_{u2} = 3.0 \qquad (15)$$

$$C_{v1} \approx C_{v3} = 1.9, \quad C_{v2} = 3.0 \qquad (16)$$

$$C_{w1} \approx C_{w3} = 1.25,\ C_{w2} = 3.0 \quad (17)$$

$$C_{T1} = 2.9, C_{T2} = 28.4, C_{T3} = 1.8 \quad (18)$$

The turbulence intensity for the three wind components ($I_u, I_v, I_w$) is directly related to their standard deviations and the wind profile. Therefore, it can be written as

$$I_j = \frac{\sigma_j}{\bar{u}} = \frac{\sigma_j / u_*}{\bar{u}/u_*} = \frac{k(\sigma_j / u_*)}{\ln\left(\frac{z-d}{z_0}\right) - \psi_m(\zeta')} \quad (19)$$

where the normalized standard deviation ($\sigma_j / u_*$) can be expressed by (8) and (10).

## 4. RESULTS

### 4.1 *Zero Plane Displacement Height (d)*

Rotach (1994) has presented the temperature variance method to estimate the zero plane displacement height ($d$) over urban surfaces. We have adopted this method to evaluate the values of $d$ from our sonic anemometer data. For details, see Huynh *et al.* (2005). Table 1 lists these estimated values for the 5 tower locations.

**Table 1.** Estimated values of $d$ (m) with respect to the wind direction for the five ARL tower locations. $N$ is the number of data points. The last line indicates the $N$ -weighted values of d for all wind directions.

| Wind Dir. (degree) | Tower #1 $d$ ( $N$ ) | Tower #2 $d$ ( $N$ ) | Tower #3 $d$ ( $N$ ) | Tower #4 $d$ ( $N$ ) | Tower#5 $d$ ( $N$ ) |
|---|---|---|---|---|---|
| 0 - 90 | 1.4 ( 44 ) | 4.7 ( 64) | 6.8 (30) | 4.8 (46) | 5.7 (57) |
| 90 - 180 | 1.7 ( 68 ) | 5.7 (106) | 1.8 (48) | 4.0 ( 49) | 4.2 (138) |
| 180 - 270 | 2.9 (253) | 5.6 (273) | 6.6 (183) | 2.5 (221) | 5.3 (186) |
| 270 - 360 | 5.3 (13) | 5.9 (16) | 5.3 (8) | 6.1 (13) | 7.4 (14) |
| 0 - 360 | 2.6 (378) | 5.5 (459) | 5.7 (269) | 3.2 (329) | 5.0 (395) |

As emphasized by Rotach (1994), the zero plane displacement ($d$) at an urban site can vary considerably with wind direction. From Table 1 we see that $d$ varies with wind direction at each location. For example, depending on wind direction, $d$ can vary from 1.4 m to 5.3 m for the Tower #1 site and from 4.7 m to 5.9 m for the Tower #2 site. Feigenwinter *et al*. (1999) have also found significant variation of $d$ values with wind direction over the city of Basel, Switzerland. These authors used eight wind direction sectors. We felt we had too few data points in some of the sectors to present a corresponding analysis here.

The reason for the significant variation of $d$ with wind direction for the five tower sites is generally understandable if we examine the significant variation of urban roughness elements (buildings, structures, and trees) with wind direction at the five sites shown in Figure 1. Fig 1(b), for example, shows that there were many more roughness elements to the west of Tower #1 than to the east. Consequently, the $d$ values are larger for westerly winds than for easterly winds. Likewise, the $d$ values are larger for the sites at Towers #2 and #5 than for the sites at Towers #1 and #4 due to the fact that the former two were more closely surrounded by taller buildings, as seen from Fig. 1 (c, f and b, e) and discussed earlier. The large values of $d$ for northeasterly and southwesterly winds (6.8 m and 6.6 m, respectively) for the Tower #3 site (Figure 1(d)) are believed to be due to the effects of the nearby trees.

The measurements by the sonic anemometers at the 5 towers do not allow us to estimate the roughness length $z_0$ for the five locations because the heights of the instruments are not high enough to be considered in the inertial (constant flux) sub-layer (Roth, 2000). Grimmond and Oke (1999) have reviewed several methods to determine the zero plane displacement height $d$ and roughness length $z_0$. A simple rule of thumb can be written as:

$$d = f_d \bar{h}\ , \quad z_0 = f_0 \bar{h} \quad (20)$$

where $\bar{h}$ is the average height of roughness elements (buildings, etc). $f_d$ and $f_0$ are two empirical coefficients. Hence,

$$z_0 = \left(\frac{f_0}{f_d}\right) d \quad (21)$$

For our later use, $f_0$ ~ 0.1 and $f_d$ ~ 0.7 have been used as a first guess. Burian *et al*. (2003) have estimated the values of $d$ and $z_0$ for the Oklahoma City downtown core area as around 13m and 2.5m, respectively, as cited by De Wekker *et al*. (2004). Because the downtown core area has taller buildings than the rest of the city, the values of $d$ and $z_0$ from Burian *et al*. are significantly larger than our estimated values for the five ARL tower sites, which are not in the downtown area.

### 4.2 Vertical *Variation of Turbulent Fluxes*

Figure 2 shows a typical diurnal variation of the turbulent kinematic heat flux ($H = \overline{w'T'}$) observed at 3 levels (10m, 5m, and 2.5m) from Tower #2 on July 29, 2003. Notice that the local time (Central Daylight Saving

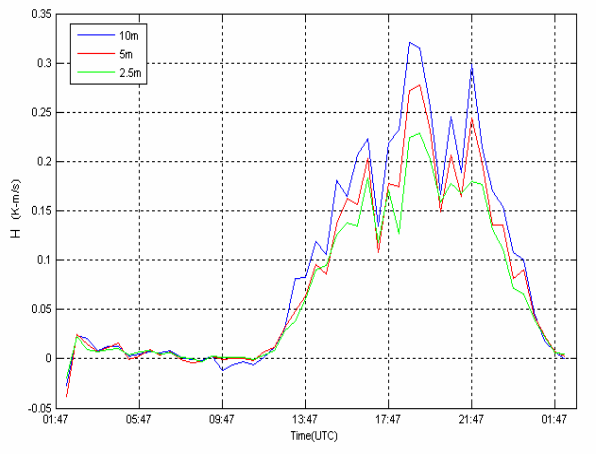


**Figure 2.** Diurnal variation of the turbulent kinematic heat flux at 10m, 5m, and 2.5m levels from Tower #2 on July 29, 2003.

Time, CDT) is 5 hours earlier than the UTC on the x axis. As expected, $H$ is usually small in the night time and early morning. In the day time, $H$ increases with time at all three levels until it reaches a maximum early afternoon. One of significant features is that $H$ increases with height from 2.5m to 5m, and from 5m to 10m during most of day time period. To further illustrate the vertical variation of $H$, scatter diagrams of $H$ between 2 levels from both Tower #2 and Tower #3 are plotted in Fig. 3. Figure 3 shows that a general trend of the increase of $H$ within the lowest 10m exists for both Tower #2 (urban area) and Tower #3 (suburban area).

Figure 4 presents the vertical variation of the averaged heat flux, $<H>$, for the 5 individual towers as well as for the 5 towers together. For these averaged heat flux plots, the reduced height ($z-d$) has been used in order to include the effect of $d$. Therefore, $<H>$ is obtained by averaging all the heat flux from a fixed value of $d$. Notice also that the results of a linear regression between y and x in each panel of both Fig. 3 and Fig. 4 are inserted. In these panels, R is the value of the corresponding correlation coefficient from the linear regressions. The positive values of the slopes of the linear regressions indicate the general trend of the increase of $H$ with the height from 2.5m to 5m, and from 5m to 10m in the roughness sub-layer.

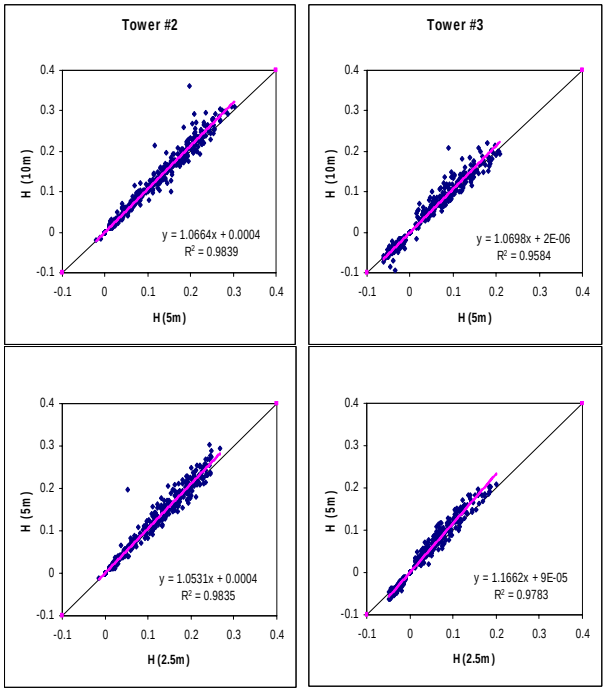


**Figure 3.** Scatter diagram of heat flux (H) between 10m and 5m (top row) and between 5m and 2.5m (bottom row) for Tower #2 and Tower #3.

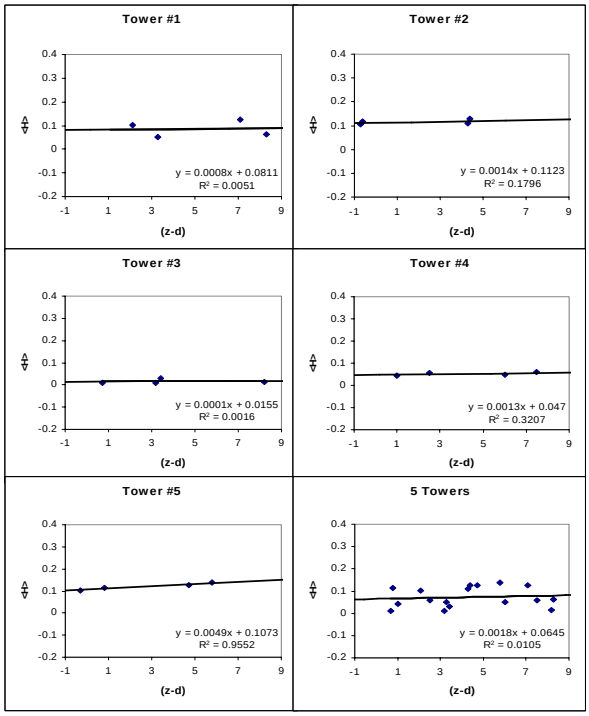


**Figure 4.** Vertical variation of averaged heat flux, <H>, for the 5 ARL towers (shown with only minimum number of data points with negative value of ($z-d$)).

Similar to Fig. 3, Figure 5 provides scatter diagrams of the friction velocity ($u_*$) between 10m and 5m as well as between 5m and 2.5m from Tower #2 and Tower #3. This figure also indicates a general trend of the increase of $u_*$ within the lowest 10m of the roughness sub-layer. This general trend of $u_*$ looks even a lot stronger than the trend for the turbulent heat flux since the positive values of the slopes of the linear regressions appear to be larger than those in Fig. 3. In

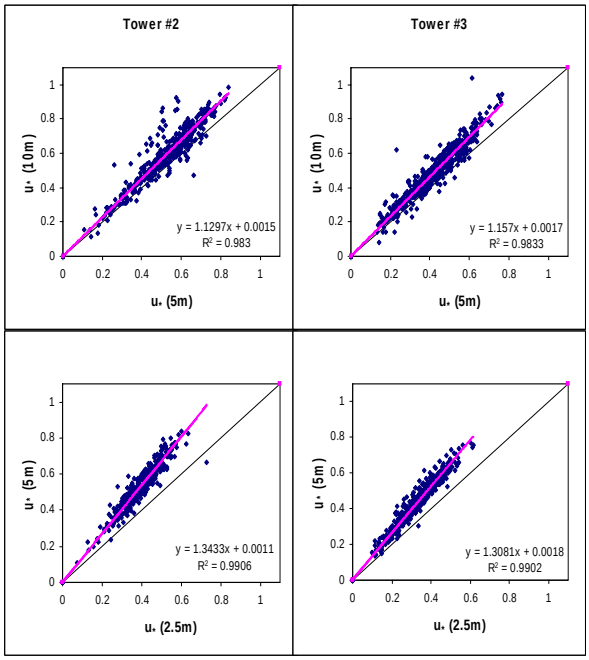


**Figure 5.** Scatter diagram of friction velocity (u*) between 10m and 5m (top row) and between 5m and 2.5m (bottom row) for Tower #2 and Tower #3.

addition, Figure 6 further shows the increase of the averaged friction velocity, $<u_*>$, with the reduced height ($z-d$) for the 5 individual towers as well as for the 5 towers together. In comparison to Figure 4, the increase of the averaged friction velocity, $<u_*>$, with ($z-d$) appears more obvious than the increase of $<H>$ with ($z-d$). Rotach (1993) has analyzed the vertical variation of Reynolds stress for the lowest few tens of meters of an urban roughness sub-layer. He found that the Reynolds stress ($u_*$) increases with height in the roughness sub-layer. Our results from the 5 tower measurements as shown by Fig. 5 and Fig. 6 appear to agree with his results.

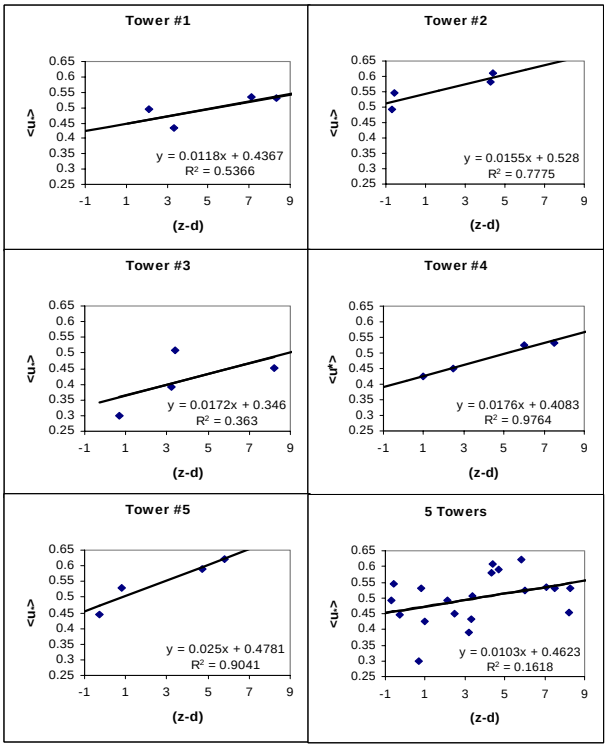


**Figure 6.** Vertical variation of averaged friction velocity, <u*>, for the 5 ARL towers.

### 4.3 *Drag Coefficient* ($C_d$)

As defined by (3), the drag coefficient ($C_d$) is a function of the measurement height ($z$), the zero plane displacement height ($d$), the roughness length ($z_0$), and the atmospheric stability ($\zeta'$). Based on the $d$ values in Table 1 and the empirical relation of (21), the variation of $C_d$ at $z$ = 10m with atmospheric stability, $(z-d)/L$, measured from 5 towers are presented in Figure 7. The solid lines in this figure express the surface layer similarity formulations of (3) – (7), in which average values of $d$ for the wind direction 90° – 180° and 180° – 270° for each tower location have been used. One of the outstanding features of Fig. 7 is the large scatter of the data points around the similarity expression (solid lines). As shown by Fig. 7, most of the measured data points are close to the neutral stratification ($\zeta' \sim 0$), say $|\zeta'| \le 0.2$. Even in this small range of $\zeta'$, the $C_d$ (10m) values are highly variable. We also have calculated $C_d$ (5m) and

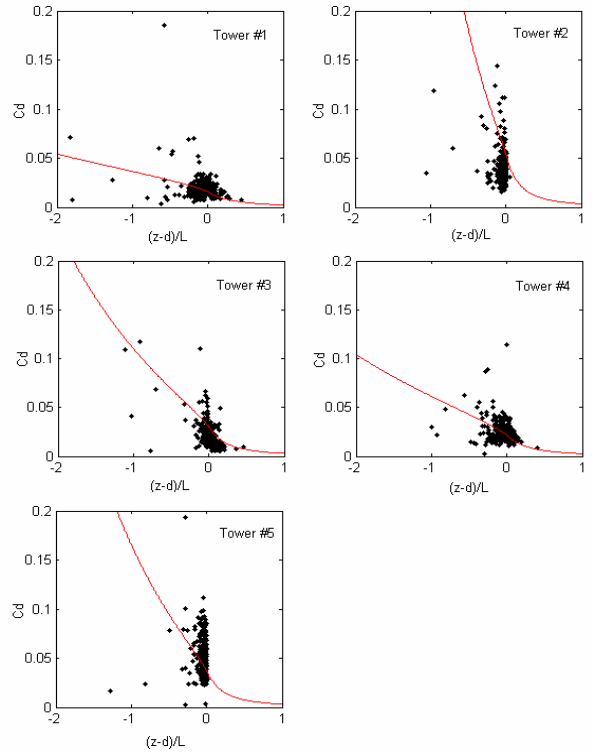


**Figure 7.** Drag coefficient, $C_d$, at 10m for the 5 ARL towers.

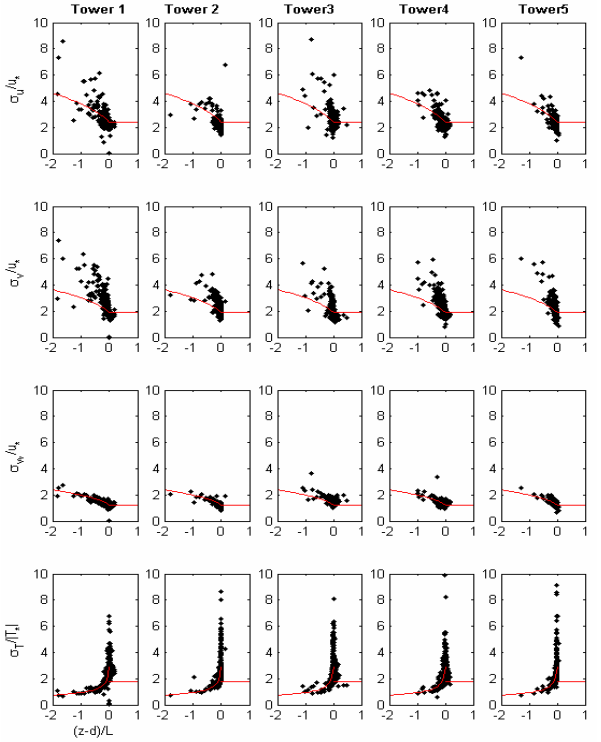


**Figure 8.** Normalized standard deviations from 5 ARL tower measurements. The lines show the empirical relations of (8) and (9) with (15), (16), (17) for ($u, v, w$) and with (18) for ($T$), respectively.

$C_d$ (2.5m) and the results from the lower levels are similar to the results from 10m level. Therefore, they are not shown here. Such large scatter of the measured data points can not be due to measurement and/or sampling errors. It can be attributed to inherent flow characteristics of the roughness sub-layer, such as transitional flow, strong wake effects, local advection, micro-scale thermals and/or large three dimensional eddies, etc..

### 4.4 *Normalized Standard Deviations*

Based on the data points ( $N$ ) weighted values of $d$ for the five tower locations in Table 1, the measured normalized standard deviations at 10m level for the three wind velocity components and for the temperature are plotted versus $(z-d)/L$ in Figure 8. The solid lines in Figure 8 represent the empirical relations of equations (8) and (9) using the empirical constants we have cited. Figure 8 shows that $\sigma_w/u_*$ (third row in Fig. 8) over Oklahoma City seems to exhibit the similar trend as over flat terrain, where $d$ in Equation (8) is close to zero. The reason is probably that the vertical velocity fluctuations are produced by small eddies, the diameters of which are of the order of the reduced height $(z-d)$ over the urban area instead of the height above the ground $(z)$ over flat terrain. In contrast, the normalized standard deviations of the horizontal wind components ( $\sigma_u/u_*$ and $\sigma_v/u_*$ ) are primarily produced by large quasi-horizontal eddies. Their diameters are typically a few hundred meters and tend to be influenced and distorted by urban buildings and trees. Consequently, $\sigma_u/u_*$ and $\sigma_v/u_*$ over an urban area are larger and more scattered as compared to their counterparts over flat terrain. The mean values of the normalized standard deviations for near-neutral conditions, defined as $|(z-d)/L| < 0.05$, are listed in Table 2. As the surface layer similarity theory suggests, the normalized standard deviations for the three wind components ( $\sigma_u/u_*$ , $\sigma_v/u_*$ , $\sigma_w/u_*$ ) under neutral conditions are "constants". From Table 2 we obtain values of 2.20, 1.84, and 1.27 when measurements from all five towers are considered. These values are very close to the corresponding values over flat terrain (Panofsky and Dutton, 1984), as indicated in Table 2. It is seen, too, that near-neutral values of these normalized standard deviations are very similar among the five tower locations.

**Table 2.** Mean values and their standard deviations (in parentheses) of the normalized standard deviations for near neutral condition defined as $|(z-d)/L| < 0.05$ measured at five ARL towers. $N$ is the number of data points.

| Tower | $N$ | $\sigma_u/u_*$ | $\sigma_v/u_*$ | $\sigma_w/u_*$ | $\sigma_T/\lvert T_*\rvert$ |
|---|---|---|---|---|---|
| No. 1 | 182 | 2.15 (0.37) | 1.80 (0.42) | 1.25 (0.21) | 2.73 (1.00) |
| No. 2 | 304 | 2.13 (0.22) | 1.93 (0.35) | 1.19 (0.10) | 2.69 (1.23) |
| No. 3 | 386 | 2.31 (0.41) | 1.84 (0.38) | 1.32 (0.14) | 2.70 (0.92) |
| No. 4 | 276 | 2.15 (0.23) | 1.84 (0.29) | 1.34 (0.12) | 2.69 (1.01) |
| No. 5 | 255 | 2.23 (0.26) | 1.73 (0.32) | 1.21 (0.11) | 2.73 (1.36) |
| All | 1403 | 2.20 | 1.84 | 1.27 | 2.71 |
| Panofsky & Dutton | | 2.39 | 1.92 | 1.25 | |

Finally, the $\sigma_T/T_*$ data are plotted using the $N$ weighted $d$ values and compared to equation (9), shown in the bottom row of Figure 8. As pointed out by Roth (2000), large variations in $\sigma_T/T_*$ are expected at near-neutral stability, where the heat flux becomes close to zero but production of temperature fluctuations does not cease. As a result of this, the estimated neutral limit values of $\sigma_T/T_*$ are dependent more on the definition of near-neutrality than on the initial choice of parameters in Equation 9, since the $d$ values only affect the $z/L$ scaling, not the magnitudes of $\sigma_T/T_*$.

### 4.5 *Turbulence Intensities*

Observational results of the average values of turbulence intensities ($I_u$, $I_v$, and $I_w$) and corresponding average wind speed are presented in Table 3. $N$ in Table 3 refers to the data points and each data point represents a half-hour (sampling time) mean. Table 3 confirms a fact that $I_u > I_v > I_w$ on average which is a common feature in the atmospheric surface layer. The ratio of $I_v/I_u$ and $I_w/I_u$ are around 90% and 55% respectively. As mentioned earlier, the locations of Tower #2 and Tower #5 can be considered as typical urban area and other three tower locations as suburban area. Table 3 also demonstrates that the turbulence intensities at the same 10m height in the urban area are significantly stronger (40% on average) than in the suburban area. The main reason for stronger turbulence intensities in urban area of Oklahoma City is the reduction (roughly 23%) of the average wind speed in the urban area as indicated in Table 3.

**Table 3.** Average values of wind speed ($\overline{u}$) and turbulence intensities ($I_u$, $I_v$, and $I_w$) at 10m AGL from the five ARL tower locations (see Fig. 1) in Oklahoma City. $N$ refers to the data points. The numbers in the parentheses denotes the standard deviations of $I_u$, $I_v$, and $I_w$ respectively.

| | $N$ | $\overline{u}$ (m/s) | $I_u$ | $I_v$ | $I_w$ |
|---|---|---|---|---|---|
| Urban | | | | | |
| Tower #2 | 446 | 3.025 | 0.454 (0.137) | 0.427 (0.142) | 0.247 (0.049) |
| Tower #5 | 380 | 2.764 | 0.518 (0.120) | 0.441 (0.154) | 0.283 (0.066) |
| Average | | | 0.486 | 0.434 | 0.265 |
| Suburban | | | | | |
| Tower #1 | 463 | 4.114 | 0.326 (0.116) | 0.319 (0.131) | 0.177 (0.039) |
| Tower #3 | 497 | 3.765 | 0.344 (0.138) | 0.269 (0.120) | 0.190 (0.056) |
| Tower #4 | 492 | 3.455 | 0.368 (0.114) | 0.347 (0.145) | 0.216 (0.039) |
| Average | | | 0.346 | 0.312 | 0.194 |

Figure 9 below shows the variation of the three turbulence intensities ($I_u$, $I_v$, and $I_w$) measured at 10m height at the five tower locations versus four wind direction sectors (0 – 90°, 90° – 180°, 180° – 270° and 270° – 360°). The plots indicate that all turbulence intensities of the three wind components vary considerably with wind direction. For example, average values of $I_u$, $I_v$, and $I_w$ measured from Tower #1 vary from one wind direction sector to another sector by as much as 87%, 90%, and 39% respectively. Figure 9 also shows the variability of $I_j$ ($j = u, v, w$) among the five locations for each wind direction sector. For example, $I_u$, $I_v$, and $I_w$ can vary 54%, 20%, and 41% respectively for the 270° – 360° wind direction sector. Such large variability in a small area of Oklahoma City appears resulting from significant heterogeneity of surface conditions as seen from Figure 1. To quantify the surface heterogeneity, one important indicator is probably the displacement height.

Figure 10 explores the possible reason for the variations of $I_j$ ($j = u, v, w$) with wind direction by linear regressions between $I_j$ and $d$. The results of linear regression in Figure 10 are:

$$I_u = 0.0382\ d + 0.2832$$

$$I_v = 0.0376\ d + 0.2495$$

$$I_w = 0.0174\ d + 0.1623$$

A larger $d$ implies a larger value of $\overline{h}$ as shown by (20), and hence a smaller relative measurement height ($z/\overline{h}$). Our results demonstrated by the three

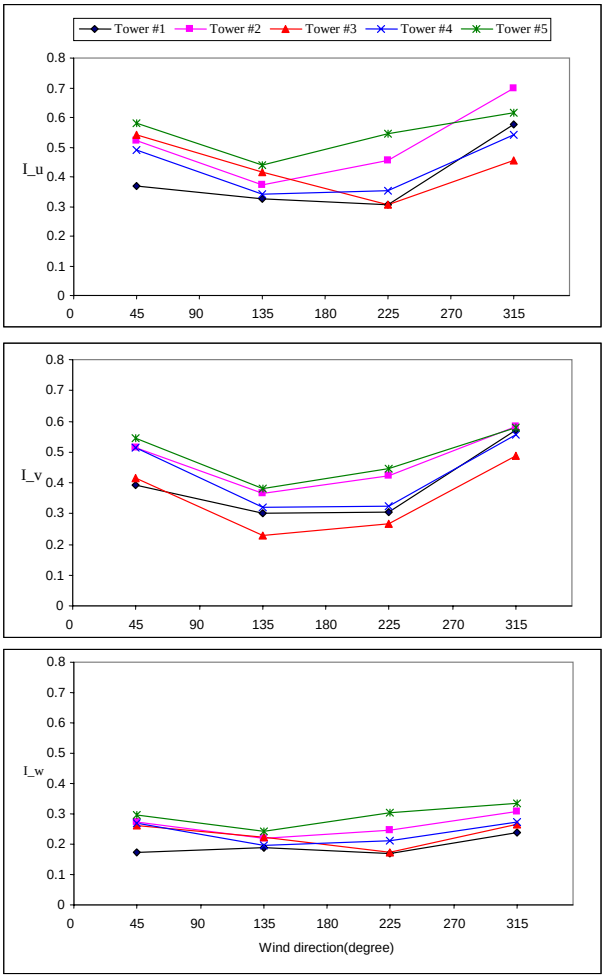


**Figure 9.** Variation of turbulence intensities with four wind sectors measured at five tower locations.

equations above and Figure 10 agree qualitatively with many previous observations (Roth, 2000, Figure 7). Therefore, the dependency of $I_j$ on wind directions results from, at least partly, the variation of $d$ with wind direction, as shown in Table 1.

One obvious feature of Figure 11 ($I_j$ vs. $(z-d)/L$) as well as Fig. 7 and Fig. 8 is the asymmetrical distribution of the data points on both sides of neutrality ($\zeta' = 0$). Most data points lied on the unstable side ($\zeta' < 0$). Especially only one data point is on the stable side ($\zeta' > 0$) for urban area locations Tower #2 and Tower #5. This phenomenon is likely due to the urban "heat island" effect. De Wekker *et al*. (2004) have discovered that the air temperature in the lower boundary layer increased about half degree after the air flow passed Oklahoma City. This implies that the lower boundary layer including the surface layer is less stable in the Oklahoma City urban area than rural area.

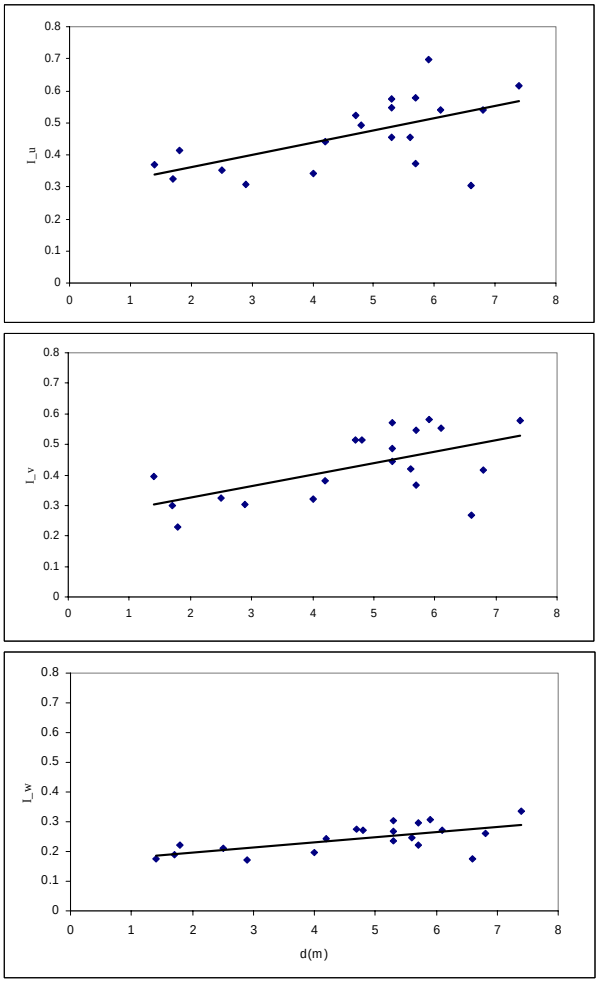


**Figure 10.** Linear regressions between Turbulence intensities and displacement height.

Figure 11 shows that all of $I_u$, $I_v$, and $I_w$ appear to decrease with increasing stability from $\zeta' = -2.0$ to $\zeta' = 1.0$. The data points, however, appear very scattered with respect to the solid empirical lines. This means that the classic Monin-Obukhov similarity theory is not applicable for the roughness sub-layer (the lower part of the surface layer).

The variable building heights and geometries, their spacing and distribution, make the wind field in the roughness sub-layer highly transitional, variable, and complex. Consequently, the turbulence statistics in this layer can hardly be expected to be described by classic Monin-Obukhov similarity theory, which has been derived for a constant flux (surface) layer. In fact, measurements of the kinematic heat and momentum fluxes at 5m and 10m on ten meter towers in JU2003 have indicated that the average fluxes at the top of the tower were more than 15% greater (up to 40% greater)

than that at the 5m level for both a suburban and an urban location (Garvey *et al*., 2004).

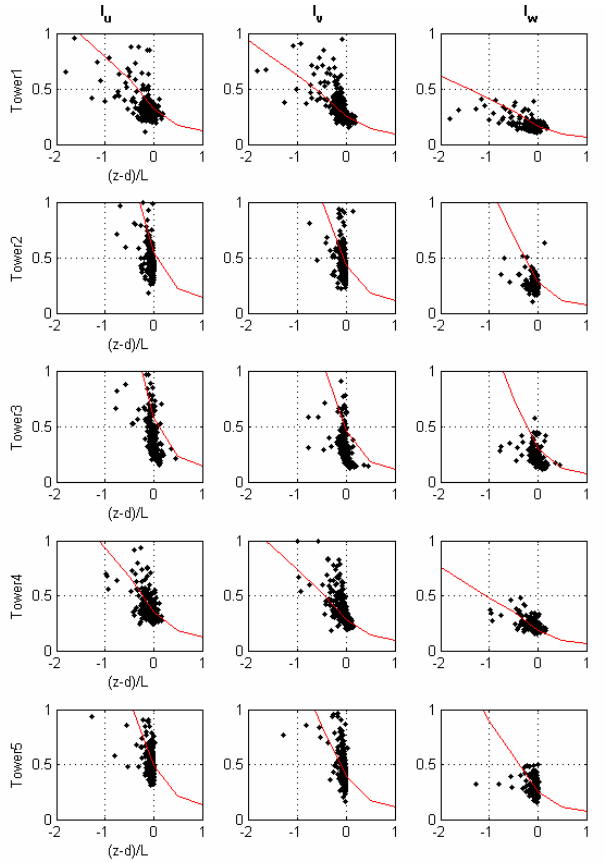


**Figure 11.** Turbulence intensities vs. $(z-d)/L$ from 5 ARL tower locations. The lines show empirical relations of Eq. (19)

Finally, the average values of the turbulence intensities for near neutral conditions, defined as $|\zeta'|$ < 0.05, from all five tower locations are plotted in Figure 12, which indicates large variations of turbulence intensities for near neutral stability. Notice that each data point in Figure 12 represents an average value of $I_j$ ( $j = u, v, w$ ) for one wind direction sector measured at one tower. Therefore, there are only 20 data points (4 wind direction sectors multiplied by 5 towers) in each plot. The wind direction sector averaging process has reduced the scatter of the data points. However, the averaged turbulence intensities still manifest increased variability at lower value of $(z-d)/z_0$ or larger value of $d$. As $(z-d)/z_0$ decreases or $d$ increases, the turbulence intensities tend to have smaller values compared to empirical relations of Equation 19 (with $\psi_m \to 0$). This further indicates the fact that similarity theory ought not to be applied even under near-neutral conditions for the roughness sub-layer.

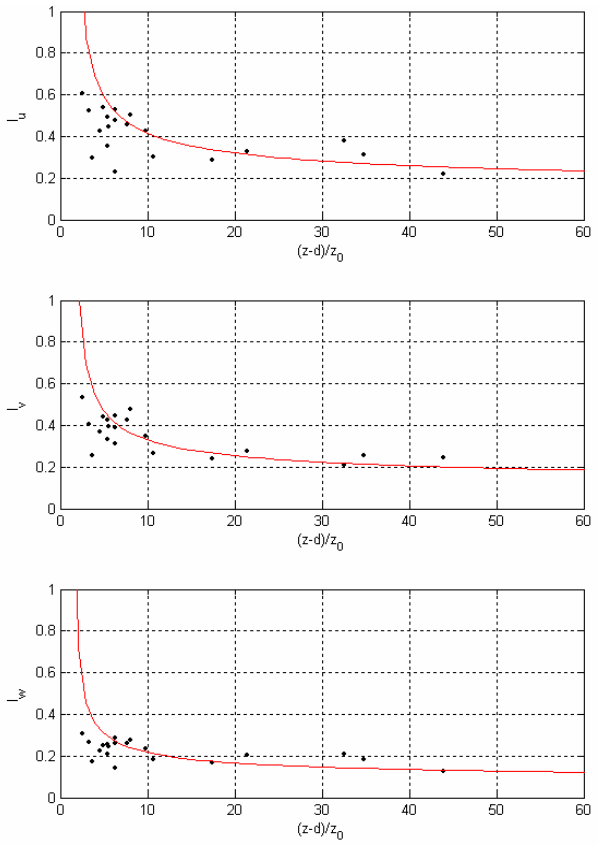


**Figure 12.** Average turbulence intensities vs. $(z-d)/z_0$ at 10m level for near neutral conditions ($|\zeta'|$ < 0.05) from 5 ARL tower locations. The lines show empirical relations of equation (19).

## 5. CONCLUSIONS

A considerable amount of sonic anemometer data from the Army Research Laboratory's five meteorological towers during the Joint Urban 2003 Oklahoma City field experiment has been collected and processed. Using the temperature variance method, the displacement heights $(d)$ for the five tower locations have been estimated. The estimated values of $d$ exhibit significant heterogeneity and depend strongly on wind direction; and so are the turbulence intensities in the roughness sub-layer.

Averaged turbulent momentum flux, $<u_*>$, and heat flux, $<H>$, appear to increase with height $(z-d)/L$ in the roughness sub-layer or the lowest part of the surface layer. Therefore, the classical concept of constant flux in the surface layer seems invalid in the roughness sub-layer. In addition, normalized standard

deviations of turbulence of $u, v, w,$ and $T$ and the turbulence intensities of $u, v$, and $w$ appear to be very scattered around Monin-Obukhov similarity formulations. It also implies that the M-O similarity or local scaling can hardly be applied to the roughness sub-layer.

## 6. ACKNOWLEDGEMENTS

We thank our colleague Young Yee of the Army Research Laboratory for many helpful discussions and for providing several useful references. We are indebted to Dean Vickers and Larry Mahrt at Oregon State University for their help for APAK software.

## 7. REFERENCES

Allwine, K.J., M. J. Leach, L. W. Stockham, J. S. Shinn, R. P. Hosker, J. F. Bowers, J. C. Pace, 2004: 'Overview of Joint Urban 2003 - An Atmospheric Dispersion Study in Oklahoma City', AMS Symposium on Planning, Nowcasting, and Forecasting in the Urban Zone, 11-15 January, Seattle, WA.

Burian, S. J., W. S. Han, and M. J. Brown, 2003: 'Morphological Analyses Using 3D Building Databases: Oklahoma City, Oklahoma'. LA-UR-, Los Alamos National Laboratory, Los Alamos, NM. 63 pp.
Chang, S.S., G.D. Huynh, C. L. Klipp, C.C. Williamson, D.M. Garvey, and Y. Wang, 2004: Observational Study of Turbulence Spectra for Joint Urban 2003. Amer. Meteor. Soc. 5th Symposium on Urban Environment, 23-27 Aug., Vancouver, BC, Canada, 3.5.

De Bruin, H. A R., Kohsek, W and Van Den Hurk, J J. M, 1993: 'A Verification of Some Methods to Determine the Fluxes of Momentum, Sensible Heat, and Water Vapour Using Standard Deviation and Structure Parameter of Scalar Meteorological Quatities'. *Boundary- Layer Meteor.*, **63**, 231-257.

De Wekker, S. F. J., L. K. Berg, K. J. Allwine, J. C. Doran, and W. J. Shaw, 2004: 'Boundary Layer Structure Upwind and Downwind of Oklahoma City During the Joint Urban 2003 Field Study'. Amer. Meteor. Soc. 5th Conf. on Urban Environment, 23-27 August, Vancouver, B. C., Canada.

Feigenwinter, C., R. Vogt, and E. Parlow, 1999: 'Vertical Structure of Selected Turbulence Characteristics above an Urban Canopy'. *Theoretical and Applied Climatology*, **62**, 51-63.

Garvey, D.M., C.L. Klipp, C.C. Williamson, G.D. Huynh, and S.S. Chang, 2004: Comparison of Surface Layer Turbulence in Urban and Suburban Domains during Joint Urban 2003. Amer. Meteor. Soc. 16th Symposium on Boundary Layers and Turbulence, 9-13 Aug., Portland, ME, 9.9.

Grimmond, C. S. B. and T. R. Oke, 1999: 'Aerodynamic Properties of Urban Areas Derived form Analysis of Surface Form'. *J. Applied Meteor.*, **38**, 1262-1292.

Huynh, G.D., S.S. Chang, C.L. Klipp, C.C. Williamson, D.M. Garvey, and Y. Wang, 2005: Spatial Variability of Turbulence Characteristics Observed during Joint Urban 2003. Amer. Meteor. Soc. ASAAQ2005 Conference, 27-29 Apr., San Francisco, CA.

Kaimal, J. C. and J. J. Finnigan, 1994: *Atmospheric Boundary Layer Flows, Their Structure and Measurement*. Oxford University Press, 289 pp.

Klipp, C. L., S. S. Chang, C. C. Williamson, G. D. Huynh, D. M. Garvey, and Y. Wang, 2004: 'A Generalized Planar Fit Method for Sonic Anemometer Tilt Correction'. 16th Symposium on Boundary Layers and Turbulence, 9-13 Aug., Portland, ME.

Lundquist, J. K., J. H. Shinn, and F. Gouveia, 2004: 'Observations of Turbulent Kinetic Energy Dissipation Rate in the Urban Environment'. 84th AMS Annual Meeting, 11-15 January, Seattle, WA.

Panofsky, H. A. and J. A. Dutton, 1984: *Atmospheric Turbulence – Models and Methods for Engineering Applications*. John Wiley and Sons, New York, 397 pp.

Rotach, M. W., 1993: 'Turbulence Close to a Roughness Urban Surface Part I: Reynolds Stress'. *Boundary-Layer Meteorology*, **65**, 1-28.

Rotach, M. W., 1994: 'Determination of the Zero Plane Displacement in an Urban Environment'. *Boundary-Layer Meteorology*, **67**, 187-193.

Roth, M., 2000: 'Review of atmospheric turbulence over cities'. *Q. J. R. Meteorol. Soc.*, **126**, p. 941-990.

Sobjan, Z., 1989: Structure of the Atmospheric Boundary Layer. Printice-Hall Inc., 317pp.

Tillman, J. E., 1972: 'The Indirect Determination of Stability, Heat and Momentum Fluxes in the Atmospheric Boundary Layer from Simple Scalar Variables during Dry Unstable Conditions'. *J. Appl. Meteorol.*, **11**, 783-792.

Vickers D., and L. Mahrt, 1997: 'Quality Control and Flux Sampling Problems from Tower and Aircraft Data'. *J. of Atmos. and Oceanic Technology*, **14**, p. 512-526.

Yee, Y., M. Bustillos, S. Chang, R. Cionco, E. Creegan, D.S. Elliott, D. Garvey, G. Huynh, D. Ligon, E. Measure, D.Quintis, M. Torres, G. Vaucher, E. Vidal, Jr., and J. Yarbrough, 2004: Wind and Turbulence Observations in Joint Urban Symposium on Planning, Nowcasting, and Forecasting in the Urban Zone, 84th AMS Annual Meeting, 11-15 January, Seattle, WA.